Mechanics and Mechanical Engineering
Vol. 21, No. 3 (2017) 569–589

Model of a Long Payload Suspended on Two Cooperating Winches and Its Preliminary Experimental Verification

Jacek Cink
Andrzej Kosucki
Lodz University of Technology
Department of Vehicles
and Fundamentals of Machine Design
jacek.cink@p.lodz.pl
andrzej.kosucki@p.lodz.pl

Received (29 May 2017)
Revised (6 August 2017)
Accepted (11 August 2017)

The dynamic model of a long payload motion in vertical plane containing the payload axis, suspended on two ropes on two co-operating winches is presented in the paper. The method of mathematical description of the model and its solving method are presented. The model is preliminary verified by comparison between simulation and experimental tests of payload oscillations done for immovable position of ropes suspension points. The results of verification and other simulation tests are presented as well.

Keywords: long payload, dynamics, overhead crane, model verification.

1. Introduction

Rationalization of exploitation process of overhead cranes and greater interest in safety and reliability, these are issues which become to be important for a payload transportation systems. Paper [11] is focused on safe transport of the payload from one point to another one without any damage of devices working under crane or injury of employees in effective and economical way. It presents payload movements on high levels (overhead) as one of methods of safe transport. Problems of payload oscillation and their minimization are described in many papers e.g. [5], [9], [13] and [20], however authors describe cases of a payload suspended on one point only. Control systems of overhead cranes with payload sway minimization are shown in papers [8] and [10]. A lot of papers, for example [14], [17], [18] and [19] present the dynamic models of laboratory devices simulating operation of overhead cranes as models of real overhead cranes. However, it is necessary to verify received solutions by experimental tests using real machine.

Overhead cranes are typical kind of underactuated systems and such they are presented in some papers e.g. [2], [15] and [16]. Authors agree, that in cases when number of system degree of freedom is higher than number of actuators (underactuated systems), analyze of kinematic and dynamic dependencies between a crane and a payload suspended on cables is necessary to develop the proper system of crane control. Crane control, proposed in these papers are developed basing on trajectory planning method, which refers to trajectory of displacement, acceleration, velocity or even jerk.

One of the methods of control with partially constant jerk called "cubic spline trajectory" (CST) is presented in [3] and compared with the method of payload sway minimization using trapezoidal control function with exactly determined periods of starting and breaking phases. Effect of payload damping, in case of CST method is reached accidently in contrary to the second method, which gives good payload sway minimization in every case by shorter duty cycle.

The most of methods mentioned in literature are presented for planar models of cranes what means for horizontal transportation, only one of mechanisms (traveling or traversing) is working. Paper [7] presents method of control of 3D overhead crane using second-order Sliding Mode Control for both mechanisms to their destination with reducing payload sway.

There are presented methods of overhead (or gantry) crane control by model predictive control (MPC) [4] and fuzzy control [12]. Proper operations of these controllers depend on the description of controlled object (overhead crane with suspended payload) by planar or 3D models, dependently on control systems.

It is obvious that a description of a tested object is the basis for dynamics research and a proper control strategies development. To the best of our knowledge, it is the first description of movement of payload suspended on two ropes system. The planar model of long payload presented in this paper is the first step to develop description of its movement in three-dimensional space.

In case of transport of a long payload, usually there are used two overhead cranes or two hoisting winches, which move in one direction. Such cases of materials transport take place especially in the stacking yards or in assembly halls, where large elements or machines are produced, or in the steel industry. This mean of transport is necessary e.g. in case of element location change during assembly works or when a long part of a machine is transported to means of transport that allows its deportation (e.g. flat wagon). Importance of this matter is testified for example by article [1], where authors write: "Bridge cranes are probably the most dangerous piece of equipment used to handle long steel products, because even the crane's smallest movements are magnified by the long payload". (..) "Two bridge cranes working in tandem to handle steel products longer than 80 feet require perfect communication between the crane operators". Issues connected with transport such kind of goods are not recognized.

In order to investigate possibilities to synchronizing the operation of two overhead cranes transporting one long payload, a model describing the motion of such kind of payload is needed. The payload is the object possessing determined mass, moment of inertia and centre of gravity and is suspended on ropes under two overhead cranes or two hoisting winches. The available literature doesn't contain information regarding the modeling of this type of the payload, so there is necessary

to develop own, verified by experiment and possibly the most useful model. The verified model of long- payload motion in vertical plane containing the payload axis is presented below. It can be used for research of a long- payload dynamics for different suspending conditions and types of input function.

According to safety rules, the simultaneous movements of traveling and traversing mechanisms are not used, so the presented model describes payload motion in one vertical plane containing the ropes suspension points and payload axis.

2. Model of the long payload

Assumptions for the model are as follows:

1. load is treated as rigid rod moving in plane motion in the vertical plane containing its axis and suspension points of ropes,

2. ropes are weightless and have any fixed length (obviously, simultaneous work of hoisting mechanisms and travelling or traversing mechanisms is forbidden),

3. wind action on the payload isn't taken into consideration,

4. input function are time runs of horizontal velocities of both ropes suspension points M and N (control functions),

5. velocities of these points don't have to be equal.

Dynamic model of long payload movement presents Fig. 1.

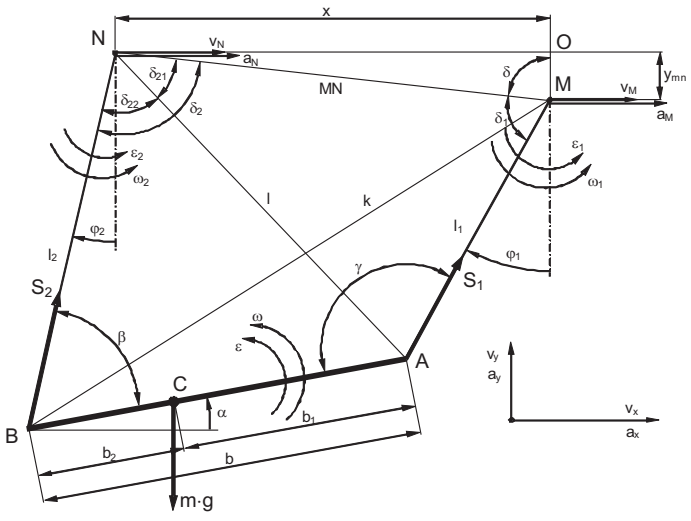

Figure 1 Dynamic model of long payload movement

In the model the following markings are assumed.
Parameters of the model:
b [m] – distance between payload suspension points A and B along the payload axis,
b_1 [m] – distance from right payload suspension point A to centre of the mass C,
b_2 [m] – distance from left payload suspension point B to centre of the mass C,
y_{MN}[m] – vertical distance between suspension points M and N,
l_1, l_2 [m] – lengths of ropes,
m [kg] – mass of the long payload,
Control variables:
v_M [m/s] – determined horizontal velocity of suspension point M,
v_N [m/s] – determined horizontal velocity of suspension point N,
a_M [m/s^2] – determined acceleration of suspension point M $\left(a_M = \frac{dv_M}{dt}\right)$,
a_N [m/s^2] – determined acceleration of suspension point N $\left(a_N = \frac{dv_N}{dt}\right)$,
x [m] – horizontal distance between points M and N $\left(\frac{dx}{dt} = v_M - v_N\right)$.
Other variables:
φ_1, φ_2 [rad] – angles of ropes inclination,
ω_1, ω_2 [1/s] – angular velocities of ropes,
ε_1, ε_2 [1/s^2] – angular accelerations of ropes,
α [rad] – angle of payload rotation,
ω [1/s] – angular velocity of payload,
ε [1/s^2] – angular acceleration of payload,
S_1 [N] – force stretching right rope,
S_2 [N] – force stretching left rope.
The model presented in Figure 1, makes possible to prescribe velocities, positions and accelerations of every element of the system as function of control variables, angular velocity ω_1 and rope inclination angle φ_1.

2.1. *Dependences of angles φ_2, α on angle φ_1*

The angle φ_1 is known as a state variable, the control variable x is known from definition as input signal. They determine completely position of payload. The angles φ_2 and α are necessary for further calculations. The geometrical dependences, taken from model presented in figure 1, can be used.
Angle δ_1 can be determined from MNO triangle:

$$\delta = \arctan\frac{y_{mn}}{x} \qquad \delta + \delta_1 + \varphi_1 = \pi \qquad \rightarrow \qquad \delta_1 = \pi - (\varphi_1 + \delta) \tag{1}$$

Angle δ_2 can be determined from MAN triangle:

$$l^2 = l_1^2 + MN^2 - 2l_1 MN\cos\delta_1 \qquad MN^2 = x^2 + y_{mn}^2 \qquad MN = \sqrt{x^2 + y_{mn}^2} \tag{2}$$

$$l_1^2 = l^2 + MN^2 - 2lMN\cos\delta_{21} \qquad \cos\delta_{21} = \frac{l^2 + MN^2 - l_1^2}{2lMN} \qquad \rightarrow \qquad \delta_{21} \tag{3}$$

Dependences from triangle NAB allow to calculate angles δ_{22} and β:

$$b^2 = l^2 + l_2^2 - 2ll_2\cos\delta_{22} \qquad \cos\delta_{22} = \frac{l^2 + l_2^2 - b^2}{2ll_2} \qquad \rightarrow \qquad \delta_{22} \tag{4}$$

$$l^2 = b^2 + l_2^2 - 2bl_2\cos\beta \qquad \cos\beta = \frac{b^2 + l_2^2 - l^2}{2bl_2} \qquad \rightarrow \qquad \beta \tag{5}$$

For angle apex N the following dependences can be written:

$$\delta_2 = \delta_{21} + \delta_{22} \qquad \frac{\pi}{2} - \delta + \delta_2 - \varphi_2 = \frac{\pi}{2} \qquad \rightarrow \qquad \varphi_2 = \delta_2 - \delta \tag{6}$$

The dependences for apex B allow to calculate angle α:

$$\beta + \varphi_2 + \alpha = \frac{\pi}{2} \quad \alpha = \frac{\pi}{2} - \beta + \delta - \delta_2 \tag{7}$$

2.2. *Dependences of angular velocities ω_2, ω on angular velocity ω_1.*

The angular velocity ω_1 and the angle φ_1 are known as a state variable, the angles φ_2 and α can be determined (chapter 2.1), the control variables v_m, v_n, x are known from definition as input signal. They let determine residual angular velocities: ω and ω_2.

Velocities of payload suspension points A and B can be expressed respectively as vector sums of ropes suspension points M and N velocities and relative velocities of points A and B to points M and N. Similarly, velocities of points A and B can be expressed respectively as vector sums of gravity centre C velocity and relative velocities of points A and B to it. The vector equations are projected on horizontal axis x and vertical one y.
Velocity of point A:

$$\bar{v}_A = \bar{v}_C + \bar{v}_{AC} \qquad v_{Ax} = v_{Cx} - b_1\omega\sin\alpha \tag{8}$$

$$v_{Ay} = v_{Cy} + b_1\omega\cos\alpha \tag{9}$$

$$\bar{v}_A = \bar{v}_M + \bar{v}_{AM} v_{Ax} = v_M + l_1\omega_1\cos\varphi_1 \tag{10}$$

$$v_{Ay} = -\,l_1\omega_1\sin\varphi_1 \tag{11}$$

After comparison of right sides of equations (8), (10) and (9), (11):

$$v_{Cx} - b_1\omega\sin\alpha = v_M + l_1\omega_1\cos\varphi_1 \tag{12}$$

$$v_{Cy} + b_1\omega\cos\alpha = -\,l_1\omega_1\sin\varphi_1 \tag{13}$$

Velocity of point B:

$$\bar{v}_B = \bar{v}_C + \bar{v}_{BC} v_{Bx} = v_{Cx} + b_2\omega\sin\alpha \tag{14}$$

$$v_{By} = v_{Cy} - b_2\omega\cos\alpha \tag{15}$$

$$\bar{v}_B = \bar{v}_N + \bar{v}_{BN} v_{Bx} = v_N + l_2\omega_2\cos\ \varphi_2 \tag{16}$$

$$v_{By} = -\,l_2\omega_2\sin\varphi_2 \tag{17}$$

After comparison of right sides of equations (14), (16) and (15), (17):

$$v_{Cx} + b_2\omega\sin\alpha = v_N + l_2\omega_2\cos\varphi_2 \tag{18}$$

$$v_{Cy} - b_2\omega\cos\alpha = -\,l_2\omega_2\sin\varphi_2 \tag{19}$$

After multiplication the equation (18) by sin φ_2 and equation (19) by cos φ_2 and after addition left and right sides angular velocity ω_2 can be eliminated.

$$v_{Cx}\sin\varphi_2 + v_{Cy}\cos\varphi_2 - b_2\omega\cos(\varphi_2+\alpha) = v_N\sin\varphi_2 \tag{20}$$

From (12) and (13) respectively velocities v_{Cx} and v_{Cy} can be determined.

$$v_{Cx} = v_M + l_1\omega_1\cos\varphi_1 + b_1\omega\sin\alpha \tag{21}$$

$$v_{Cy} = -\,l_1\omega_1\sin\varphi_1 - b_1\omega\cos\alpha \tag{22}$$

After multiplication the equation (21) by sin φ_2 and equation (19) by cos φ_2 and after addition left and right sides.

$$v_{Cx}\sin\varphi_2 + v_{Cy}\cos\varphi_2 = v_M\sin\varphi_2 - l_1\omega_1\sin(\varphi_1-\varphi_2) - b_1\omega\cos(\varphi_2+\alpha) \tag{23}$$

After replacing (23) to (20):

$$\begin{aligned} &v_M\sin\varphi_2 - l_1\omega_1\sin(\varphi_1-\varphi_2) - b_1\omega\cos(\varphi_2+\alpha) - b_2\omega\cos(\varphi_2+\alpha)\\ &= v_N\sin\varphi_2 \end{aligned} \tag{24}$$

After ordering:

$$(v_M - v_N)\sin\varphi_2 - l_1\omega_1\sin(\varphi_1-\varphi_2) = b\omega\cos(\varphi_2+\alpha) \tag{25}$$

From dependence (25) angular velocity ω can be calculated

$$\omega = \frac{(v_M - v_N)\sin\varphi_2 - l_1\omega_1\sin(\varphi_1-\varphi_2)}{b\cos(\varphi_2+\alpha)} \tag{26}$$

Using the theorem about projection velocities of two points (A and B) of rigid body on straight line connecting these point.

$$v_{Ax}\cos\alpha + v_{Ay}\sin\alpha = v_{Bx}\cos\alpha + v_{By}\sin\alpha \tag{27}$$

The equations (10) and (16) can be multiplied by cos α, equations (11) and (17) by sin α.

$$v_{Ax}\cos\alpha = v_M\cos\alpha + l_1\omega_1\cos\varphi_1\cos\alpha \tag{28}$$

$$v_{Ay}\sin\alpha = -\,l_1\omega_1\sin\varphi_1\sin\alpha \tag{29}$$

$$v_{Bx}\cos\alpha = v_N\cos\alpha + l_2\omega_2\cos\varphi_2\cos\alpha \tag{30}$$

$$v_{By}\sin\alpha = -\,l_2\omega_2\sin\varphi_2\sin\alpha \tag{31}$$

Formulas (28), (29), 30), (31) can be used in (27):

$$\begin{aligned} &v_M\cos\ \alpha + l_1\omega_1\cos\ \varphi_1\cos\ \alpha - l_1\omega_1\sin\ \varphi_1\sin\ \alpha\\ &= v_N\cos\ \alpha + l_2\omega_2\cos\ \varphi_2\cos\ \alpha - l_2\omega_2\sin\ \varphi_2\sin\ \alpha \end{aligned} \tag{32}$$

After ordering:

$$v_M\cos\alpha + l_1\omega_1\cos(\varphi_1+\alpha) = v_N\cos\alpha + l_2\omega_2\cos\ (\varphi_2+\alpha) \tag{33}$$

From (33) the angular velocity ω_2 can be calculated.

$$\omega_2 = \frac{(v_M - v_N)\cos\ \alpha + l_1\omega_1\cos\ (\varphi_1+\alpha)}{l_2\cos\ (\varphi_2+\alpha)} \tag{34}$$

2.3. *Dependences of angular acceleration ε_1 on angular velocities ω_1, ω_2 and ω.*

The angular velocity ω_1 and the angle φ_1 are known as a state variable, the angles φ_2 and α can be determined (chapter 2.1), the angular velocities ω_2 and ω can be determined (chapter 2.2), the control variables v_M, v_N, a_M, a_N, x are known from definition. They let determine demanded angular acceleration ϵ_1 as derivative ω_1 in relation to time t ($\mathrm{d}\omega_1/\mathrm{dt}$).

Accelerations of payload suspension points A and B can be expressed respectively as vector sums of ropes suspension points M and N accelerations and relative accelerations (tangent and normal) of points A and B to points M and N. Similarly, accelerations of points A and B can be expressed respectively as vector sums of gravity centre C acceleration and relative accelerations (tangent and normal) of points A and B to it. The vector equations are projected on horizontal axis x and vertical one y.
Acceleration of point A:

$$\bar{a}_A = \bar{a}_C + \bar{a}^t_{AC} + \bar{a}^n_{AC} a_{Ax} = a_{Cx} - b_1\varepsilon \sin\ \alpha - b_1\omega^2 \cos\ \alpha \tag{35}$$

$$a_{Ay} = a_{Cy} + b_1\varepsilon \cos\ \alpha - b_1\omega^2 \sin\ \alpha \tag{36}$$

$$\bar{a}_A = \bar{a}_M + \bar{a}^t_{AM} + \bar{a}^n_{AM} a_{Ax} = a_M + l_1\varepsilon_1 \cos\ \varphi_1 + l_1\omega_1^2 \sin\ \varphi_1 \tag{37}$$

$$a_{Ay} = -\ l_1\varepsilon_1 \sin\ \varphi_1 + l_1\omega_1^2 \cos\ \varphi_1 \tag{38}$$

After comparison of right sides equations (35), (37) and (37), (38):

$$a_{Cx} - b_1\varepsilon \sin\ \alpha - b_1\omega^2 \cos\ \alpha = a_M + l_1\varepsilon_1 \cos\ \varphi_1 + l_1\omega_1^2 \sin\ \varphi_1 \tag{39}$$

$$a_{Cy} + b_1\varepsilon \cos\ \alpha - b_1\omega^2 \sin\ \alpha = -\ l_1\varepsilon_1 \sin\ \varphi_1 + l_1\omega_1^2 \cos\ \varphi_1 \tag{40}$$

Acceleration of point B:

$$\bar{a}_B = \bar{a}_C + \bar{a}^t_{BC} + \bar{a}^n_{BC} a_{Bx} = a_{Cx} + b_2\varepsilon \sin\ \alpha + b_2\omega^2 \cos\ \alpha \tag{41}$$

$$a_{By} = a_{Cy} - b_2\varepsilon \cos\ \alpha + b_2\omega^2 \sin\ \alpha \tag{42}$$

$$\bar{a}_B = \bar{a}_N + \bar{a}_{BN} + \bar{a}^n_{BN} a_{Bx} = a_N + l_2\varepsilon_2 \cos\ \varphi_2 + l_2\omega_2^2 \sin\ \varphi_2 \tag{43}$$

$$a_{By} = -\ l_2\varepsilon_2 \sin\ \varphi_2 + l_2\omega_2^2 \cos\ \varphi_2 \tag{44}$$

After comparison of right sides equations (41), (43) and (42), (44):

$$a_{Cx} + b_2\varepsilon \sin\ \alpha + b_2\omega^2 \cos\ \alpha = a_N + l_2\varepsilon_2 \cos\ \varphi_2 + l_2\omega_2^2 \sin\ \varphi_2 \tag{45}$$

$$a_{Cy} - b_2\varepsilon \cos\ \alpha + b_2\omega^2 \sin\ \alpha = -\ l_2\varepsilon_2 \sin\ \varphi_2 + l_2\omega_2^2 \cos\ \varphi_2 \tag{46}$$

After multiplication the equation (45) by sin φ_2 and equation (46) by cos φ_2 and after addition left and right sides angular acceleration ε_2 is eliminated.

$$\begin{aligned} &a_{Cx} \sin\ \varphi_2 + a_{Cy} \cos\ \varphi_2 - b_2\varepsilon \cos\ (\varphi_2 + \alpha) + b_2\omega^2 \sin\ (\varphi_2 + \alpha) \\ &= a_N \sin\ \varphi_2 + l_2\omega_2^2 \end{aligned} \tag{47}$$

From (39) and (40) respectively accelerations a_{Cx} and a_{Cy} can be determined.

$$a_{Cx} = a_M + l_1\varepsilon_1 \cos\ \varphi_1 + l_1\omega_1^2 \sin\ \varphi_1 + b_1\varepsilon \sin\ \alpha + b_1\omega^2 \cos\ \alpha \tag{48}$$

$$a_{Cy} = -\ l_1\varepsilon_1 \sin\ \varphi_1 + l_1\omega_1^2 \cos\ \varphi_1 - b_1\varepsilon \cos\ \alpha + b_1\omega^2 \sin\ \alpha \tag{49}$$

After multiplication the equation (48) by sin φ_2 and equation (49) by cos φ_2 and after addition left and right sides the equation can be adapted to equation (47).

$$\begin{aligned} &a_{Cx} \sin\ \varphi_2 + a_{Cy} \cos\ \varphi_2 \\ &= a_M \sin\ \varphi_2 - l_1\varepsilon_1 \sin\ (\varphi_1 - \varphi_2) + l_1\omega_1^2 \cos\ (\varphi_1 - \varphi_2) \\ &-b_1\varepsilon \cos\ (\varphi_2 + \alpha) + b_1\omega^2 \sin\ (\varphi_2 + \alpha) \end{aligned} \tag{50}$$

Formula (50) can be used in (47):

$$\begin{aligned} &a_M \sin\ \varphi_2 - l_1\varepsilon_1 \sin\ (\varphi_1 - \varphi_2) + l_1\omega_1^2 \cos\ (\varphi_1 - \varphi_2) \\ &-b_1\varepsilon \cos\ (\varphi_2 + \alpha) + b_1\omega^2 \sin\ (\varphi_2 + \alpha) \\ &-b_2\varepsilon \cos\ (\varphi_2 + \alpha) + b_2\omega^2 \sin\ (\varphi_2 + \alpha) \\ &= a_N \sin\ \varphi_2 + l_2\omega_2^2 \end{aligned} \tag{51}$$

After ordering:

$$\begin{aligned} &(a_M - a_N) \sin\ \varphi_2 - l_1\varepsilon_1 \sin\ (\varphi_1 - \varphi_2) + \\ &+l_1\omega_1^2 \cos\ (\varphi_1 - \varphi_2) + b\omega^2 \sin\ (\varphi_2 + \alpha) -\ l_2\omega_2^2 \\ &= b\varepsilon \cos\ (\varphi_2 + \alpha) \end{aligned} \tag{52}$$

From (52) the angular acceleration ϵ can be calculated (ϵ depends on ϵ_1).

$$\begin{aligned} \varepsilon = &\frac{(a_M - a_N) \sin\ \varphi_2 - l_1\varepsilon_1 \sin\ (\varphi_1 - \varphi_2) + l_1\omega_1^2 \cos\ (\varphi_1 - \varphi_2)}{b \cos\ (\varphi_2 + \alpha)} \\ &+\frac{b\omega^2 \sin\ (\varphi_2 + \alpha) -\ l_2\omega_2^2}{b \cos\ (\varphi_2 + \alpha)} \end{aligned} \tag{53}$$

The Newton law for payload motion can be determined. The vector equation of motion can be projected on horizontal axis x and vertical axis y.

$$m\bar{a} = \bar{S}_1 + \bar{S}_2 + m\bar{g} \qquad ma_{cx} = S_1 \sin\ \varphi_1 + S_2 \sin\varphi_2 \tag{54}$$

$$ma_{cy} = S_1 \cos\varphi_1 + S_2 \cos\varphi_2 - mg \tag{55}$$

$$I_C\varepsilon = S_1 b_1 \cos\ (\varphi_1 + \alpha)\ - S_2 b_2 \cos\ (\varphi_2 + \alpha) \tag{56}$$

After multiplication (54) by cos φ_2 and (55) by sin φ_2 and after subtraction left and right sides the force S_2 can be eliminated.

$$m\,(a_{cx} \cos\ \varphi_2 - a_{cy} \sin\ \varphi_2) = S_1 \sin\ (\varphi_1 - \varphi_2) + mg \sin\ \varphi_2 \tag{57}$$

After multiplication (54) by cos φ_1 and (55) by sin φ_1 and after subtraction left and right sides the force S_1 can be eliminated.

$$m\,(a_{cx} \cos\ \varphi_1 - a_{cy} \sin\ \varphi_1) = -\ S_2 \sin\ (\varphi_1 - \varphi_2) + mg \sin\ \varphi_1 \tag{58}$$

From (57) and (58) respectively forces S_1 and S_2 can be determined.

$$S_1 = \frac{m\left(a_{cx}\cos\ \varphi_2 - a_{cy}\sin\ \varphi_2\right) - mg\sin\ \varphi_2}{\sin\ (\varphi_1 - \varphi_2)} \tag{59}$$

$$S_2 = -\ \frac{m\left(a_{cx}\cos\ \varphi_1 - a_{cy}\sin\ \varphi_1\right) - mg\sin\ \varphi_1}{\sin\ (\varphi_1 - \varphi_2)} \tag{60}$$

The dependences (59) and (60) can be used in (56).

$$\begin{array}{l} I_C\varepsilon = \frac{m(a_{cx}\cos\ \varphi_2 - a_{cy}\sin\ \varphi_2) - mg\sin\ \varphi_2}{\sin\ (\varphi_1 - \varphi_2)} b_1\cos\ (\varphi_1 + \alpha) \\ + \frac{m(a_{cx}\cos\ \varphi_1 - a_{cy}\sin\ \varphi_1) - mg\sin\ \varphi_1}{\sin\ (\varphi_1 - \varphi_2)} b_2\cos\ (\varphi_2 + \alpha) \end{array} \tag{61}$$

Using formulas (48) and (49) the expressions in brackets in (48) can be determined.

After multiplication (48) and (49) respectively by $\cos\ \varphi_2$ and $\sin\ \varphi_1$ and after subtraction left and right sides:

$$\begin{array}{l} a_{Cx}\cos\ \varphi_2 - a_{Cy}\sin\ \varphi_2 = \\ = a_M\cos\ \varphi_2 + l_1\varepsilon_1\cos\ (\varphi_1 - \varphi_2) + l_1\omega_1^2\sin\ (\varphi_1 - \varphi_2) \\ + b_1\varepsilon\sin\ (\varphi_2 + \alpha) + b_1\omega^2\cos\ (\varphi_2 + \alpha) \end{array} \tag{62}$$

After multiplication (48) and (49) respectively by $\cos\ \varphi_1$ and $\sin\ \varphi_1$ and after subtraction left and right sides:

$$\begin{array}{l} a_{Cx}\cos\ \varphi_1 - a_{Cy}\sin\ \varphi_1 \\ a_M\cos\ \varphi_1 + l_1\varepsilon_1 + b_1\varepsilon\sin\ (\varphi_1 + \alpha) + b_1\omega^2\cos\ (\varphi_1 + \alpha) \end{array} \tag{63}$$

Using formulas (62) and (63) in (61):

$$\begin{array}{l} I_C\varepsilon = \left[\frac{m\left(a_M\cos\ \varphi_2 + l_1\varepsilon_1\cos\ (\varphi_1 - \varphi_2) + l_1\omega_1^2\sin\ (\varphi_1 - \varphi_2)\right)}{\sin\ (\varphi_1 - \varphi_2)}\right. \\ \quad \left. + \frac{m\left(b_1\varepsilon\sin\ (\varphi_2 + \alpha) + b_1\omega^2\cos\ (\varphi_2 + \alpha)\right)}{\sin\ (\varphi_1 - \varphi_2)}\right] b_1\cos\ (\varphi_1 + \alpha) \\ \quad - \frac{mg\sin\ \varphi_2}{\sin\ (\varphi_1 - \varphi_2)} b_1\cos\ (\varphi_1 + \alpha) \\ \quad + \left[\frac{m(a_M\cos\ \varphi_1 + l_1\varepsilon_1 + b_1\varepsilon\sin\ (\varphi_1 + \alpha))}{\sin\ (\varphi_1 - \varphi_2)}\right. \\ \quad \left. + \frac{mb_1\omega^2\cos\ (\varphi_1 + \alpha)}{\sin\ (\varphi_1 - \varphi_2)}\right] b_2\cos\ (\varphi_2 + \alpha) \\ \quad - \frac{mg\sin\ \varphi_1}{\sin\ (\varphi_1 - \varphi_2)} b_2\cos\ (\varphi_2 + \alpha) \end{array} \tag{64}$$

The second dependence between angular accelerations ϵ and ϵ_1 is determined.

After using (53) in (64) and ordering, the equation with one unknown ϵ_1 is formulated.

$$
\begin{aligned}
&-l_1\varepsilon_1 \left[\begin{array}{l} \frac{I_C}{m}\sin\ (\varphi_1-\varphi_2)\sin\ (\varphi_1-\varphi_2) \\ +bb_1\cos\ (\varphi_1-\varphi_2)\cos\ (\varphi_1+\alpha)\cos\ (\varphi_2+\alpha) \\ -b_1^2\sin\ (\varphi_1-\varphi_2)\cos\ (\varphi_1+\alpha)\sin\ (\varphi_2+\alpha) \\ +bb_2\cos\ (\varphi_2+\alpha)\cos\ (\varphi_2+\alpha) \\ -b_1b_2\sin\ (\varphi_1-\varphi_2)\sin\ (\varphi_1+\alpha)\cos\ (\varphi_2+\alpha) \end{array} \right] \\
&= \ a_M b \left[\begin{array}{l} b_1\cos\ (\varphi_1+\alpha)\cos\ (\varphi_2+\alpha)\cos\ \varphi_2 \\ +b_2\cos\ \varphi_1\cos\ (\varphi_2+\alpha)\cos\ (\varphi_2+\alpha) \end{array} \right] \\
&-(a_M-a_N) \left[\begin{array}{l} \frac{I_C}{m}\sin\ (\varphi_1-\varphi_2)\sin\ \varphi_2 \\ -b_1^2\cos\ (\varphi_1+\alpha)\sin\ (\varphi_2+\alpha)\sin\ \varphi_2 \\ -b_1b_2\sin\ (\varphi_1+\alpha)\cos\ (\varphi_2+\alpha)\sin\ \varphi_2 \end{array} \right] \\
&-l_1\omega_1^2 \left[\begin{array}{l} \frac{I_C}{m}\sin\ (\varphi_1-\varphi_2)\cos\ (\varphi_1-\varphi_2) \\ -bb_1\sin\ (\varphi_1-\varphi_2)\cos\ (\varphi_1+\alpha)\cos\ (\varphi_2+\alpha) \\ -b_1^2\cos\ (\varphi_1-\varphi_2)\cos\ (\varphi_1+\alpha)\sin\ (\varphi_2+\alpha) \\ -b_1b_2\cos\ (\varphi_1-\varphi_2)\sin\ (\varphi_1+\alpha)\cos\ (\varphi_2+\alpha) \end{array} \right] \\
&+l_2\omega_2^2 \left[\begin{array}{l} \frac{I_C}{m}\sin\ (\varphi_1-\varphi_2)\ -b_1^2\cos\ (\varphi_1+\alpha)\sin\ (\varphi_2+\alpha) \\ -b_1b_2\sin\ (\varphi_1+\alpha)\cos\ (\varphi_2+\alpha) \end{array} \right] \\
&-b\omega^2 \left[\begin{array}{l} \frac{I_C}{m}\sin\ (\varphi_1-\varphi_2)\sin\ (\varphi_2+\alpha) \\ -b_1^2\cos\ (\varphi_1+\alpha)\sin\ (\varphi_2+\alpha)\sin\ (\varphi_2+\alpha) \\ -b_1^2\cos\ (\varphi_1+\alpha)\cos\ (\varphi_2+\alpha)\cos\ (\varphi_2+\alpha) \\ -b_1b_2\sin\ (\varphi_1+\alpha)\sin\ (\varphi_2+\alpha)\cos\ (\varphi_2+\alpha) \\ -b_1b_2\cos\ (\varphi_1+\alpha)\cos\ (\varphi_2+\alpha)\ \cos\ (\varphi_2+\alpha) \end{array} \right] \\
&-gb[b_1\cos\ (\varphi_1+\alpha)\ \sin\ \varphi_2\cos\ (\varphi_2+\alpha) \\
&+b_2\sin\ \varphi_1\cos\ (\varphi_2+\alpha)\cos\ (\varphi_2+\alpha)]
\end{aligned} \tag{65}
$$

For simplification there is comfortably to introduce the following new coefficients:

$$
E = \ -l_1 \left[\begin{array}{l} \frac{I_C}{m}\sin\ (\varphi_1-\varphi_2)\sin\ (\varphi_1-\varphi_2) \\ +bb_1\cos\ (\varphi_1-\varphi_2)\cos\ (\varphi_1+\alpha)\cos\ (\varphi_2+\alpha) \\ -b_1^2\sin\ (\varphi_1-\varphi_2)\cos\ (\varphi_1+\alpha)\sin\ (\varphi_2+\alpha) \\ +bb_2\cos\ (\varphi_2+\alpha)\cos\ (\varphi_2+\alpha) \\ -b_1b_2\sin\ (\varphi_1-\varphi_2)\sin\ (\varphi_1+\alpha)\cos\ (\varphi_2+\alpha) \end{array} \right] \tag{66}
$$

$$
AM = \ b \left[\begin{array}{l} b_1\cos\ (\varphi_1+\alpha)\cos\ (\varphi_2+\alpha)\cos\ \varphi_2 \\ +b_2\cos\ \varphi_1\cos\ (\varphi_2+\alpha)\cos\ (\varphi_2+\alpha) \end{array} \right] \tag{67}
$$

$$
AMN = -\left[\begin{array}{l} \frac{I_C}{m}\sin(\varphi_1-\varphi_2)\sin\varphi_2 - b_1^2\cos(\varphi_1+\alpha)\sin(\varphi_2+\alpha)\sin\varphi_2 \\ -b_1b_2\sin(\varphi_1+\alpha)\cos(\varphi_2+\alpha)\sin\varphi_2 \end{array} \right] \tag{68}
$$

$$
\Omega 1 = \ -l_1 \left[\begin{array}{l} \frac{I_C}{m}\sin\ (\varphi_1-\varphi_2)\cos\ (\varphi_1-\varphi_2) \\ -bb_1\sin\ (\varphi_1-\varphi_2)\cos\ (\varphi_1+\alpha)\cos\ (\varphi_2+\alpha) \\ -b_1^2\cos\ (\varphi_1-\varphi_2)\cos\ (\varphi_1+\alpha)\sin\ (\varphi_2+\alpha) \\ -b_1b_2\cos\ (\varphi_1-\varphi_2)\sin\ (\varphi_1+\alpha)\cos\ (\varphi_2+\alpha) \end{array} \right] \tag{69}
$$

$$
\Omega 2 = \ l_2 \left[\begin{array}{l} \frac{I_C}{m}\sin\ (\varphi_1-\varphi_2)\ -b_1^2\cos\ (\varphi_1+\alpha)\sin\ (\varphi_2+\alpha) \\ -b_1b_2\sin\ (\varphi_1+\alpha)\cos\ (\varphi_2+\alpha) \end{array} \right] \tag{70}
$$

$$\Omega = \; -b \begin{bmatrix} \frac{I_C}{m} \sin\,(\varphi_1 - \varphi_2) \sin\,(\varphi_2 + \alpha) \\ -b_1^2 \cos\,(\varphi_1 + \alpha) \sin\,(\varphi_2 + \alpha) \sin\,(\varphi_2 + \alpha) \\ -b_1^2 \cos\,(\varphi_1 + \alpha) \cos\,(\varphi_2 + \alpha) \cos\,(\varphi_2 + \alpha) \\ -b_1 b_2 \sin\,(\varphi_1 + \alpha) \sin\,(\varphi_2 + \alpha) \cos\,(\varphi_2 + \alpha) \\ -b_1 b_2 \cos\,(\varphi_1 + \alpha) \cos\,(\varphi_2 + \alpha)\, \cos\,(\varphi_2 + \alpha) \end{bmatrix} \tag{71}$$

$$G = \; -gb \begin{bmatrix} b_1 \cos\,(\varphi_1 + \alpha)\, \sin\,\varphi_2 \cos\,(\varphi_2 + \alpha) \\ +b_2 \sin\,\varphi_1 \cos\,(\varphi_2 + \alpha) \cos\,(\varphi_2 + \alpha) \end{bmatrix} \tag{72}$$

Angular acceleration ε_1 can be determined as follows:

$$E\varepsilon_1 = \; AMa_M + AMN\,(a_M - a_N)\; + \Omega 1\omega_1^2\; + \Omega 2\omega_2^2\; + \Omega\omega^2\; + G \tag{73}$$

$$\varepsilon_1 = \frac{AMa_M + AMN\,(a_M - a_N)\; + \Omega 1\omega_1^2\; + \Omega 2\omega_2^2\; + \Omega\omega^2\; + G}{E} \tag{74}$$

2.4. *Mathematical description of the system*

All factors and variables in formula (74) describing $\varepsilon_1 = \frac{d^2\varphi_1}{dt^2} = \ddot{\varphi}_1$ are dependent only on angle φ_1, angular velocity $\omega_1 = \frac{d\varphi_1}{dt} = \dot{\varphi}_1$ and input control signals $\mathbf{u} = [\mathrm{v}_M, \mathrm{v}_N, \mathrm{a}_M, \mathrm{a}_N, \mathrm{x}]$ so mathematical description of the system can be presented in general form:

$$\ddot{\varphi}_1 = f\;(\varphi_1,\, \dot{\varphi}_1,\, \mathrm{u}) \tag{75}$$

However, authors prefer other form of mathematical description of the system called the state variables space notation. It demands to determine the state variables connected with the system and describing its behaviour. For the described model the angular velocity of rope 1 ω_1 and angle of rope 1 inclination φ_1 are chosen as the state variables. The mathematical description in space of state variables has form of first order differential equations system:

$$\begin{array}{l} \frac{d\omega_1}{dt} = \frac{AMa_M + AMN(a_M - a_N)\; + \Omega 1\omega_1^2\; + \Omega 2\omega_2^2\; + \Omega\omega^2\; + G}{E} \\ \frac{d\varphi_1}{dt} = -\omega_1 \end{array} \tag{76}$$

In general:

$$\begin{array}{l} \frac{d\omega_1}{dt} = f_1\;(\omega_1,\, \varphi_1,\, \mathrm{u}) \\ \frac{d\varphi_1}{dt} = f_2\;(\omega_1,\, \varphi_1,\, \mathrm{u}) \end{array} \tag{77}$$

The equations are solved by numerical method of integration – Euler method where initial conditions are defined dependently on the initial state of the system. To solve this model the special program written in the integrated development environment based on Free Pascal compiler is developed.

Although, the right side of first equation in (76), (77) is relatively complicated the modern computers calculate them very quickly.

3. Model verification

To experimental verification of the long payload model, the overhead crane (span 10 m and hoisting capacity 5t) and jib crane (range 6m and hoisting capacity 500 kg) are used. Both devices and example long payload (crane boom) are presented in Fig. 2.

Figure 2 Location of devices used for verification

Schema of stand for model verification is presented in Fig. 2.

Both devices are equipped with potentiometric measurement systems of payload sway, using one-rotational potentiometers connected by joints with sliding clamps cooperating with ropes. These systems ensure independent measurement of payload sway in directions of respectively luffing and slewing and bridge and carriage movements.

Strength meter (range to 500 N) allows register the initial horizontal force the payload is unbalanced with.

The verification is carried out by immovable both rope suspension points what allows record demanded parameters without disturbances such as inaccurate mapping of speed by drive systems of the overhead crane and jib crane.

For comparison the real and simulated values the payload is deflected from the equilibrium position and oscillations of the payload are recorded.

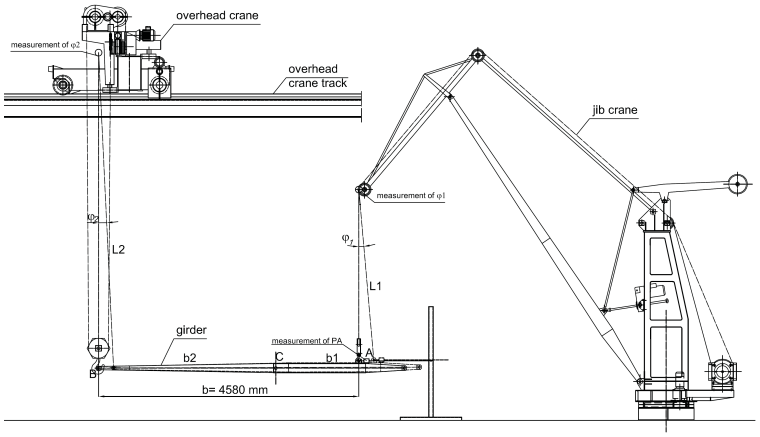

Figure 3 Schema of stand for long payload model verification

Parameters of the stand are:

l_1 , l_2 – rope lengths suspended respectively under jib crane and overhead crane,

b_1, b_2 – location of the centre of gravity C of investigated girder,

m – mass of the girder.

The following output variables are registered:

φ_1 – angle of jib crane ropes sway in luffing direction,

φ_2 – angle of overhead crane ropes sway in bridge motion direction,

PA – initial horizontal force that makes payload outbalanced.

On the basis of time runs of φ_1 and φ_2 the runs of ω_1, ω_2, α and ω can be calculated:

ω_1 – angular velocity of jib crane ropes in vertical plane including payload axis,

ω_2 – angular velocity of overhead crane ropes in vertical plane including payload axis,

ω – angle of payload rotation in vertical plane,

α – angular velocity of payload rotation in vertical plane.

Verification of the model takes place during the cycle (130 s duration) of free oscillations (velocities of ropes suspension points M and N are equal zero) of the system with different lengths of ropes (different levels of payload suspension). Presented waveforms are average ones values from measured series, whereas theoretical runs are the response to the identical input control signals as in real system. The angles and velocities described above are compared to verify the model.

Indexes "s" and "e" mean respectively simulation and experimental runs. Exampled waveforms for the lowest level of payload suspension are presented in Figs. 4, 5 and 6.

The momentary deviations of each values calculated as the difference between the measured values and simulation ones are determined as well.

$$\Delta\omega = \omega_{pom} - \omega_s \quad [\text{rad/s}] \tag{78}$$

$$\Delta\omega = \omega_{pom} - \omega_s \quad [^o] \tag{79}$$

$$\Delta\alpha = \alpha_{pom} - \alpha_s \quad [^o] \tag{80}$$

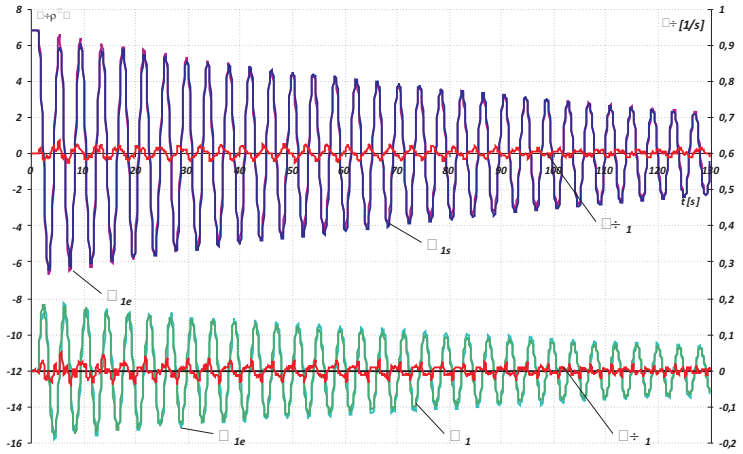

Figure 4 Comparison of simulation and experimental runs of angle φ_1, velocity ω_1 and deviations $\Delta\varphi_1$ and $\Delta\omega_1$

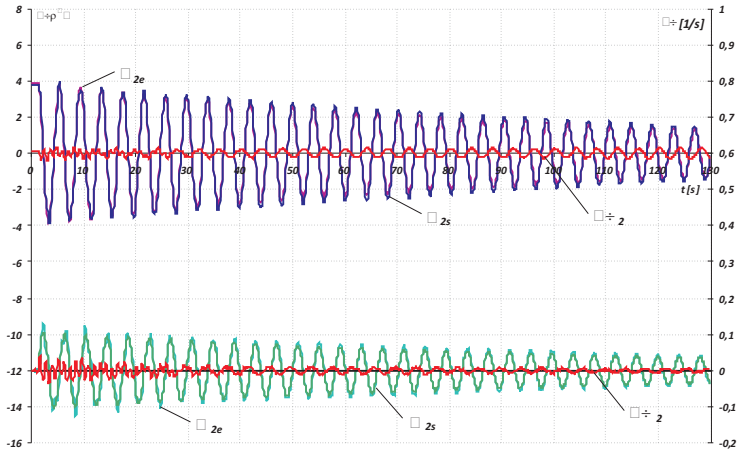

Figure 5 Comparison of simulation and experimental runs of angle φ_2, velocity ω_2 and deviations $\Delta\varphi_2$ and $\Delta\omega_2$

These research show high compatibility of the model with real system, both in the range of the vibration frequency and the amplitude of each variable. To proof this, the comparison of each angle waveform at the beginning and in the end of the cycle is presented in Figs. 7 and 8.

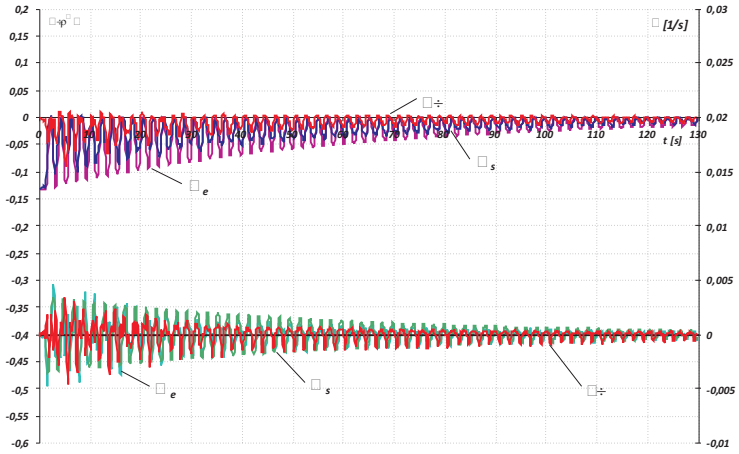

Figure 6 Comparison of simulation and experimental runs of angle α, velocity ω and deviations $\Delta\alpha$ and $\Delta\omega$

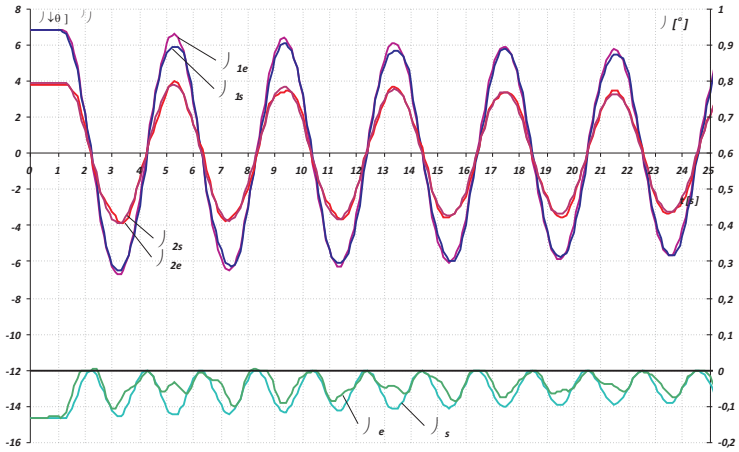

Figure 7 Comparison of simulation and experimental runs of angles α, φ_1 and φ_2 at the beginning of the cycle

Coefficients of model accuracy for each value are introduced and defined below:

$$W\omega = \frac{\frac{\sum_{i=1}^{n}|\Delta x|}{n}}{x_{\max} - x_{\min}} 100\% \tag{81}$$

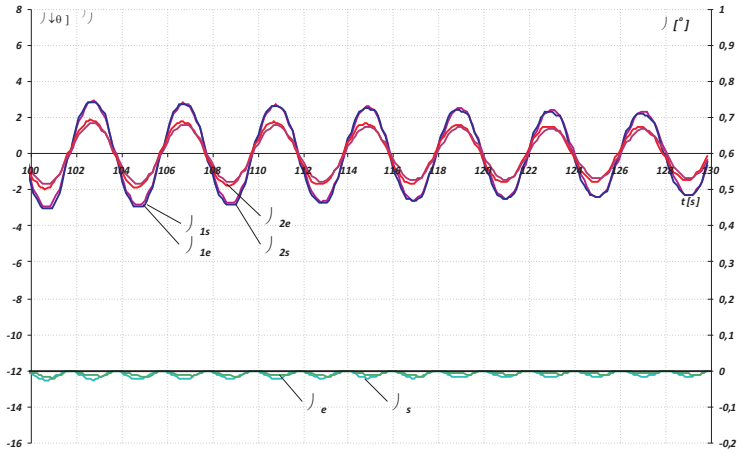

Figure 8 Comparison of simulation and experimental runs of angles α, φ_1 and φ_2 in the end of the cycle

where:

x – compared values,

n – number of samples in one measuring cycle.

Coefficients calculated according to formula above have values of a few (1,36 - 6,76) percent dependently on different levels of payload suspension.

4. Simulation tests

The presented model, its solution and verification provides the basis for its using in the future research of dynamics and methods of generation of an input functions to reach desirable operational effects e.g. possibilities of fast transport of long payload with its sway damping. Preliminary simulation studies of long payload for different control functions $v_M(\mathrm{t})$ and $v_N(\mathrm{t})$ of suspension points to determine the behavior of the payload subjected to various inputs have already been performed.

Due to possibilities of different displacements of suspension points the value of displacement differences is introduced and calculated as follows:

$$\Delta_x = s_M - s_N \tag{82}$$

where:

Δ_x [m] – difference between displacements of suspension points M and N,

s_M [m] – horizontal displacement of point M

s_N [m] – horizontal displacement of point N

The chosen waveforms for different times of acceleration and deceleration phases of points M and N are presented in Fig. 9. The velocities of points M and N are not equal and different from zero. The accelerations of points M and N are different during acceleration and deceleration phases. The different values (during duty cycle) of the angles φ_1 i φ_2 are visible. The angle α is different to zero. It is caused by different ropes length.

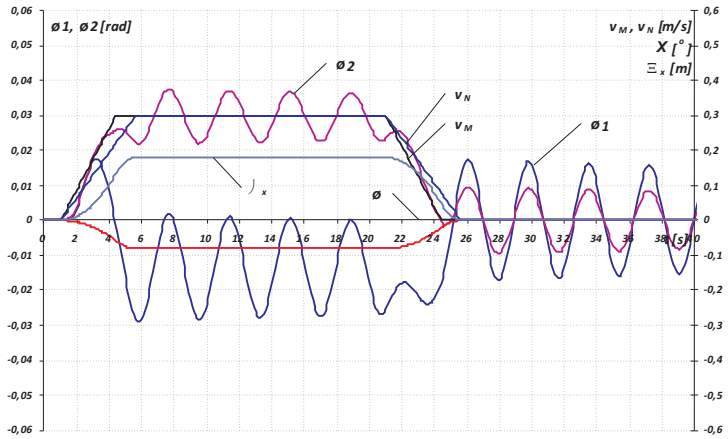

Figure 9 Results of simulation tests for different acceleration and deceleration times of points M and N. The case of different ropes length

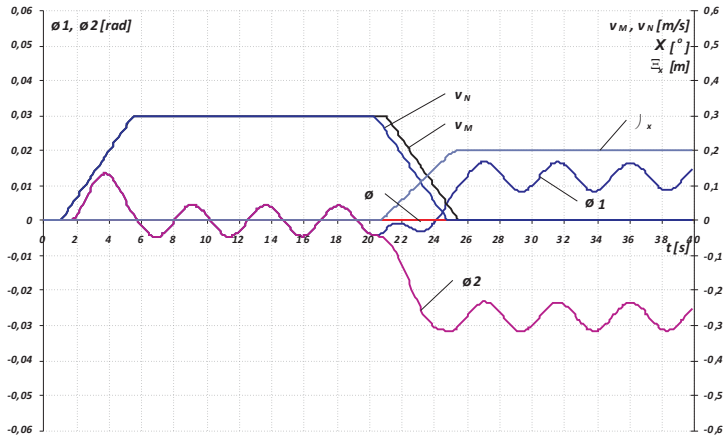

Figure 10 Results of simulation tests for different displacements of points M and N

The results of simulation tests for different displacements of points M and N, respectively $s_M = 64$ m and $s_N = 5,8$ m in case of equal ropes length ($l_1 = l_2 = 5$ m) are presented in Fig. 10. At the end of the cycle, the angles of ropes are different and stabilize on levels depending on centre of the gravity location C, defined by parameters b_1 and b_2.

Fig. 11 shows one of tested methods of payload oscillation minimization when the times of acceleration and deceleration phases are calculated near periods of

oscillations of mathematical pendulum ($t_r = t_h = 4,5$ s) with length equal length of ropes $l_1 = l_2 = 5$ m. This method is based on method described in [6] and used for sway minimization of payload suspended on one point.

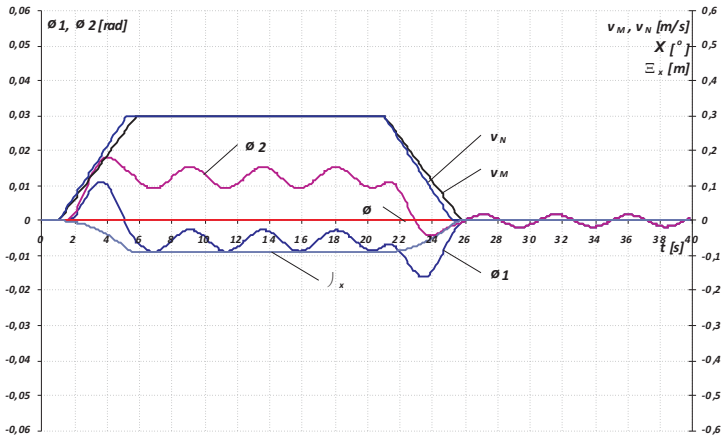

Figure 11 Results of simulation tests for different acceleration and deceleration times of points N and M. The case of equal ropes length

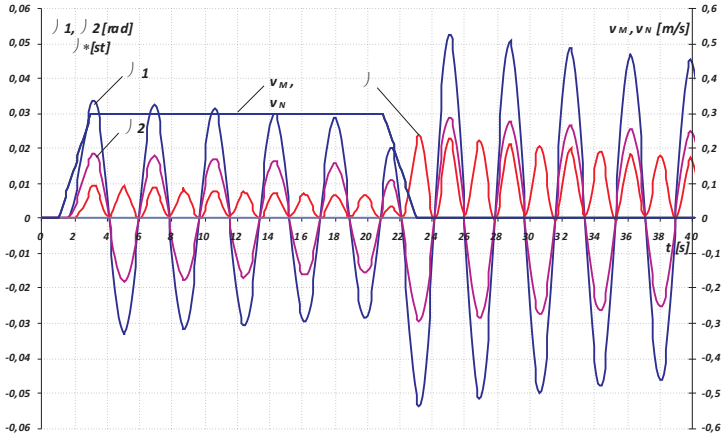

Figure 12 Results of simulation tests for minimum acceleration and deceleration times of points M and N. The case of different ropes length

In this case oscillations at the end of duty cycle are smaller than one centimeter. For comparison when the times of acceleration and deceleration phases are $t_r = t_h = 3$ s amplitude of oscillations at the end of cycle reaches 15 cm.

Figures 12 and 13 confirm usefulness of method of sway minimization basing on trapezoidal function. Figure 12 shows case of long payload suspended on ropes with different lengths when the times of acceleration and deceleration are minimal due to the absence of slip. Figure 13 presents the same object controlled by velocities of points M and N with acceleration and deceleration times equal the average of periods of oscillations of mathematical pendulums with lengths l_1 and l_2.

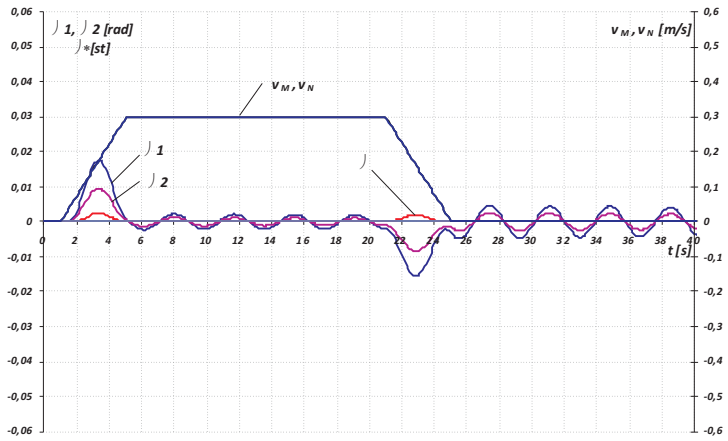

Figure 13 Results of simulation tests for acceleration and deceleration times of points M and N equal the average of periods of oscillations of mathematical pendulums with lengths l_1 and l_2. The case of different ropes length

Comparison of payload sway angles at the end of the duty cycle shows minimizing of payload swaying about 85% in case presented in figure 13 with respect to case in Fig. 12. The time of duty cycle in figure 13 is less then 2 seconds longer than the shortest one (Fig. 12).

5. Conclusions

The model of long payload suspended on two points in one vertical plane is presented. The model describes the most often way of long payload transport. The preliminary experimental verification gives satisfactory results. The model is easy to solve and let realize necessary simulation tests. Preliminary tests of the described model show possibilities of using different control functions for better payload transport. It is planned to apply the modified method of trapezoidal and other more complex input functions to control a long payload movement with sway limitation. The trapezoidal function used for payload swing minimization is described in [6] and [3].

The next planned steps are: to develop methods of payload oscillation minimization, to develop the model of long payload motion to three-dimensional space. It let develop the system which allows transport long payload fast, safe and without oscillations.

References

[1] **Alesia, J.**: Handling Long Steel Products Proves to Be a Balancing Act, Iron & Steel Technology - *Safety First*, 38–39, **2011**.

[2] **Chen He, Fang Yongchun and Sun Ning**: A Novel Optimal Trajectory Planning Method for Overhead Cranes with Analytical Expressions. *Proceedings of the 33rd Chinese Control Conference*, Nanjing, China, **2014**.

[3] **Cink, J. and Kosucki, A.**:The selected methods of driving mechanisms shaping in order to minimize payload sway, *Problems of Working Machines Development, Kosucki A., Monographs of Lodz University of Technology,* Lodz, 51–64, **2015**.

[4] **Jolevski, D. and Bego O.**: Model predictive control of gantry/bridge crane with anti-sway algorithm. *Journal of Mechanical Science and Technology*, 29, 2, 827–834, **2015**.

[5] **Ho-Hoon Lee** : A New Motion-Planning Scheme for Overhead Cranes With High-Speed Hoisting, *Journal of Dynamic Systems, Measurement, and Control* JUNE, 126, 359–364, **2004**.

[6] **Kosucki, A.**: Badanie transportu ładunków przy wykorzystaniu skojarzonych ruchów mechanizmów suwnic pomostowych (Loads transport research using associated movements of overhead cranes mechanisms). *Rozprawy Naukowe. Politechnika Łódzka, 74; Zeszyty Naukowe. Politechnika Łódzka* no. 1175, WPŁ, Łódź, **2013**.

[7] **Le Anh Tuan, Hoang Manh Cuong and Soon-Geul Lee**: Second-order Sliding Mode Control of 3D Overhead Cranes. *International Journal of Precision Engineering and Manufacturing*, 15, 5, 811–819, **2014**.

[8] **Lifu Wang, Xiangdong Wang and Zhi Kong**: Anti-swing Control of Overhead Cranes, *Proceedings of the 6th World Congress on Intelligent Control and Automation*, Dalian, China, 8024–8028, **2006**.

[9] **Maneeratanaporn Jadesada and Murakami Toshiyuki**: Anti-sway Sliding-mode with Trolley Disturbance Observer for Overhead Crane system, *The 12th IEEE International Workshop on Advanced Motion Control*, Sarajevo, Conference Publications, 1–6, **2012**.

[10] **Rigoberto Toxqui, Wen Yu and Xiaoou Li**: Anti-swing control for overhead crane with neural compensation, *International Joint Conference on Neural Networks*, Vancouver, BC, Canada, 4697–4703, **2006**.

[11] **Rogers, L. K.**: Overhead handling equipment basics, *Modern Materials Handling*, 12, 30–34, **2011**.

[12] **Smoczek, J. and Szpytko, J.**: Iterative and Evolutionary Optimization for Interval Analysis-based Designing a Fuzzy Controller for a Planar Crane Model. *19th International Conference On Methods and Models in Automation and Robotics*, MMAR, 258–263, **2014**.

[13] **Vazquez, C. and Collado, J.**: Oscillation attenuation in an overhead crane: Comparison of some approaches, *6th International Conference on Electrical Engineering, Computing Science and Automatic Control,CCE*, Conference Publications, 1–6, **2009**.

[14] **Wahyudi, Jamaludin Jalani, Riza Muhida and Momoh Jimoh Emiyoka Salami**: Control Strategy for Automatic Gantry Crane Systems: A Practical and Intelligent Approach, *International Journal of Advanced Robotic Systems*, 4, 4, 447–456, **2007**.

[15] **Wu Xianqing, He Xiongxiong and Sun Ning**: An Analytical Trajectory Planning Method for Underactuated Overhead Cranes with Constraints. *Proceedings of the 33rd Chinese Control Conference,* July 28-30, Nanjing, China, **2014**.

[16] **Xuebo Zhang, Yongchun Fang and Ning Sun**: Minimum-Time Trajectory Planning for Underactuated Overhead Crane Systems With State and Control Constraints. *IEEE Transactions On Industrial Electronics*, Vol. 61, No. 12, December **2014**.

[17] **Yang Jung Hua and Yang Kuang Shine**: Adaptive coupling control for overhead crane systems, *Mechatronics*, 17, 143–152, **2007**.

[18] **Yang, J. H. and Yang, K. S.**: Adaptive Control for 3-D Overhead Crane Systems, *Proceedings of the 2006 American Control Conference, Minneapolis*, Minnesota, USA, June 14-16, 1832–1837, **2006**.

[19] **Yang, J. H.**: On the Adaptive Tracking Control of 3-D Overhead Crane Systems, *Adaptive Control*, 277–306, **2009**.

[20] **Zhengyan Zhang, Dingfang Chen and Min Feng**: Dynamics Model and Dynamic Simulation of Overhead Crane Load Swing Systems Based on the ADAMS, *Computer-Aided Industrial Design and Conceptual Design*, CAID/CD 2008, 9th International, Conference Publications, 484–487, **2008**.